JOURNAL OF GUIDANCE, CONTROL, AND DYNAMICS
Vol. 17, No. 5, September–October 1994

Cost of Model Reference Adaptive Control: Analysis, Experiments, and Optimization

R. S. Messer,* R. T. Haftka,† and H. H. Cudney‡
Virginia Polytechnic Institute and State University, Blacksburg, Virginia 24061

In this paper a study of the performance of model reference adaptive control is presented in numerical simulations and verified experimentally on a single-degree-of-freedom system with the objective of understanding how differences between the plant and the reference model affect the maximum control force and control effort performance metrics. These performance metrics were found to be highly sensitive to differences between the plant and the reference model. It was also found that when such differences exist, lowering the required performance by reducing the required damping actually increases the maximum force and control effort for a single-degree-of-freedom example. Optimization of weighting matrices is shown to help reduce the increases in these performance metrics. However, the optimization results in a design that, for successful realization, requires a sampling frequency 40–80 times the Nyquist frequency.

Introduction

DURING the past decade, researchers have shown much interest in control and identification of large space structures (LSSs). Our inability to model these LSSs accurately has generated extensive research into controllers capable of maintaining stability in the presence of large structural uncertainties as well as changing structural characteristics. Adaptive controllers are seen as one possible solution. Most of the research on adaptive controllers has been theoretical in nature,[1–5] and experimental verification[6–9] is lagging behind. In addition, the focus of most theoretical research has been on designing stable adaptive controllers with little concern for the issues of control effort.

In the present work we consider model reference adaptive control (MRAC), which employs an idealized reference model and forces the actual structure to behave like the reference model.[1] Although it is possible to design an adaptive controller based on a poor model of a structure and still achieve stability and performance, apparently no one has examined the effects on the required control effort. Previous researchers[2] have chosen the reference model to be a reduced model of the actual structure with the same frequencies and mode shapes and some additional damping. Whereas this would be the ideal situation, having an exact analytical model is not probable. Therefore we have intentionally introduced differences between our reference model and the actual plant (structure) model. The objectives of this paper are to 1) study the performance of MRAC in numerical simulations and verify experimentally how differences between the plant and reference model affect the performance metrics, maximum control force, and total control effort and 2) minimize the effects of these differences by optimizing the control design.

MRAC is applied, both numerically and experimentally, to a simple structural system that has a high-fidelity model, so differences between the reference model and plant can be controlled and adjusted. Performance metrics are developed and monitored to determine the effects of differences on the maximum force and control effort. To minimize the effects of differences on the performance metrics, available weighting matrices are optimized. However, the optimization is considered useful only if experimental results show the same improvement trends.

Received Aug. 17, 1992; revision received Oct. 4, 1993; accepted for publication Jan. 10, 1994.

*Graduate Project Assistant, Department of Aerospace and Ocean Engineering; currently Engineer/Scientist Specialist, McDonnell Douglas Aerospace. Member AIAA.

†Christopher Kraft Professor, Department of Aerospace and Ocean Engineering. Associate Fellow AIAA.

‡Assistant Professor, Department of Mechanical Engineering. Member AIAA.

This paper begins with a short review of the MRAC algorithm. Next, control effort indices are defined, followed by a discussion of steps taken in implementation of the integration algorithm to ensure the simulation mimics the experiments. An example is introduced and experimental and analytical results presented for reference models with varying amounts of error. Finally, the weighting matrices used in MRAC are optimized to reduce the effects of error between the reference model and the plant.

Model Reference Adaptive Control

MRAC is one of the more popular adaptive control methods[1–8] that does not require system identification. In MRAC, controller gains are adjusted so the actual system response becomes the response of an ideal reference model. Because this reference model can be of lower order than a model of the actual system, this method is very attractive for application to LSSs, where structural models can be of very high order and require truncation for use with practical controllers. Figure 1 shows a block diagram of a generalized MRAC system.[2]

Problem Formulation

We consider the large class of linear, time-invariant stable systems of the form

$$\dot{X}_p(t) = A_p X_p(t) + B_p U_p(t) \tag{1a}$$

$$Y_p(t) = C_p X_p(t) \tag{1b}$$

It is assumed A_p and B_p are controllable, A_p and C_p are observable, and the number of inputs U_p is equal to the number of output measurements Y_p. A stable reference model is similarly described,

$$\dot{X}_m(t) = A_m X_m(t) + B_m U_m(t) \tag{2a}$$

$$Y_m = C_m X_m(t) \tag{2b}$$

The degree to which the actual plant response follows the reference model response is measured by an error vector e_y, defined as

$$e_y(t) = Y_m(t) - Y_p(t) \tag{3}$$

where Y_m and Y_p are the output vectors of the reference model and the plant, respectively. The objective of MRAC is to force e_y to zero asymptotically.

Adaptive Control Law

The MRAC law used in this paper is based on the work of Sobel et al.[1] and is summarized briefly here. The control input U_p is written as

$$U_p(t) = K(t)r(t) \tag{4}$$

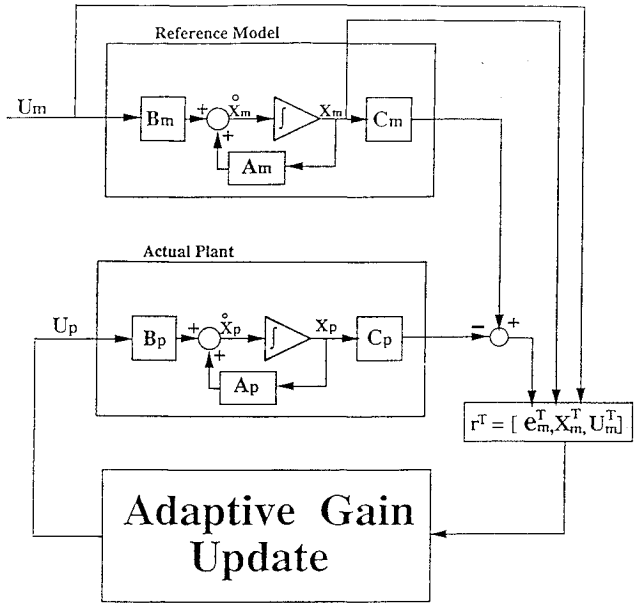

Fig. 1 Model reference adaptive control block diagram.[2]

where

$$r^T = [e_y^T, X_m^T, U_m^T] \tag{5a}$$

and the gain matrix K is composed of a proportional and an integral component

$$K(t) = K_{\text{pr}}(t) + K_I(t) \tag{5b}$$

The adaptive laws for the gains $K_{\text{pr}}(t)$ and $K_I(t)$ are given as

$$K_{\text{pr}}(t) = e_y r^T T^* \tag{6a}$$

$$\dot{K}_I(t) = e_y r^T T \tag{6b}$$

where T^* and T are time-invariant weighting matrices of appropriate dimension chosen by the designer. Sufficient conditions for global stability are presented by Sobel et al.[1] and summarized by Boussalis et al.[10] For LSSs, sufficient requirements for stability are nonzero inherent damping and collocated sensors and actuators. In the present work MRAC was implemented with collocated velocity sensors and force actuators.

Performance Metrics

In order to quantify increases or decreases in the performance of MRAC when differences between the reference model and the actual system exist, the following procedure was adopted. First, a baseline linear model representing the actual system is chosen. Next, a reference model is chosen with a specified amount of difference from the baseline model. The effect of this difference on the control effort is quantified by the following two performance metrics: 1) the maximum control force required from each actuator $(1, \ldots, M)$,

$$U^i_{\max} = \max(|U^i(t)|) \qquad 0 \le t \le t_{\text{final}} \qquad i = 1, \ldots, M \tag{7}$$

and 2) the control effort (CE),

$$\text{CE} = \sqrt{\int U^T U \, dt} \tag{8}$$

Here CE is the traditional measure of control cost related to energy consumption; $U_{\max}$ is a more hardware-related measure that may indicate voltage, power, or actuator force requirements.

Correlating Experiment and Simulation

To accurately model the exchange of force and velocity information between the digital controller and the actual structure, integration of reference model equations [Eqs. (2a) and (2b)] and gain equations [Eq. (6b)] was uncoupled from integration of the actual structure equations [Eqs. (1a) and (1b)]. While integration of the two sets of equations must be uncoupled, their responses are highly coupled through exchange of velocity input and force output information. To ensure this exchange of information was modeled correctly, the following steps were taken in the simulation:

Step 1. At $t = t_0$ velocities of both the reference model and actual plant are stored, and used in Eqs. (3–6), to calculate control forces $U_p[t_0]$.

Step 2. The states of the reference model [Eqs. (2a) and (2b)] and integral gains [Eq. (6b)] are calculated at $t = t_0 + \Delta t$, where Δt is the controller sampling time interval.

Step 3. Control forces $U_p[t_0]$ are applied while the equations of the actual structure are integrated to $t = t_0 + \Delta t$.

Note that the velocities of the actual plant and the control forces calculated in step 1 are kept fixed during steps 2 and 3. In this way the digital effects of the controller on the actual system are simulated. The integration process was a third-order Euler implicit scheme with Newton iteration, selected for achieving good accuracy at low computational cost.

Suspended-Mass Example

Model of Physical System

MRAC is applied to the suspended-mass system shown in Fig. 2. The mass is suspended by four equal-length wires 0.025 in. in diameter. These wires are connected to the mass and the supporting structure with $\frac{3}{16}$-in. eye-screws that are used to adjust the tension in the wires. The base of the support structure is an aluminum plate ($24 \times 24 \times 3/8$ in.) connected to the wires by four right-angle steel connectors. The analytical model of this system is a standard spring-mass-damper system, where the spring constant k is proportional to the tension in the wires. The equation of motion for the system is

$$m\ddot{x}(t) + c\dot{x}(t) + kx(t) = u(t) \tag{9}$$

and the state-space representation is

$$\begin{bmatrix} \dot{x}_{1p} \\ \dot{x}_{2p} \end{bmatrix} = \begin{bmatrix} -2\zeta_p\omega_{np} & -\omega_{np}^2 \\ 1.0 & 0 \end{bmatrix} \begin{bmatrix} x_{1p} \\ x_{2p} \end{bmatrix} + \begin{bmatrix} \frac{1}{m} \\ 0 \end{bmatrix} u_p(t) \tag{10}$$

where x_{1p} and x_{2p} are velocity and displacement, respectively. Using free response data, the natural frequency was found to be 5.95 Hz, and inherent damping was estimated to be $\zeta_p = 0.0006$.

Reference Model

The state-space representation of the reference model is similar to the actual system except the control force is set to zero so that the reference model follows a free damped response,

$$\begin{bmatrix} \dot{x}_{1m} \\ \dot{x}_{2m} \end{bmatrix} = \begin{bmatrix} -2\zeta_m\omega_{nm} & -\omega_{nm}^2 \\ 1.0 & 0.0 \end{bmatrix} \begin{bmatrix} x_{1m} \\ x_{2m} \end{bmatrix} \tag{11}$$

The behavior of the system is primarily described by its natural frequency, and differences between the two systems are introduced by varying the natural frequency of the reference model by

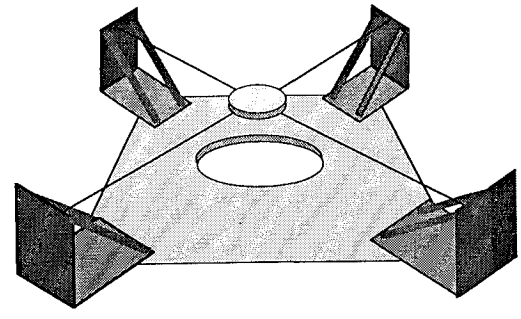

Fig. 2 Drawing of the suspended-mass system.

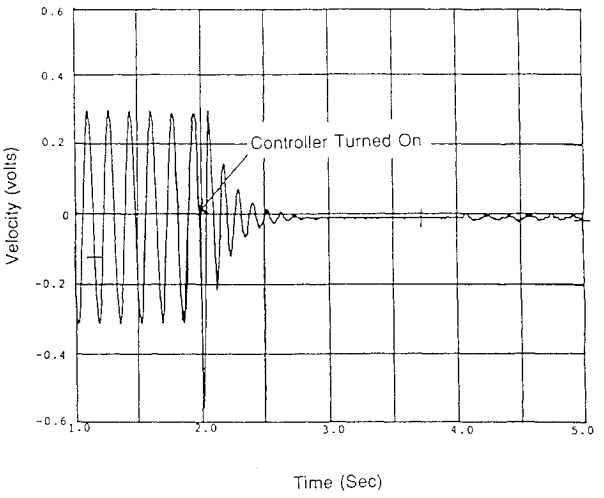

Fig. 3 Experimental velocity response; reference model frequency is 150% of plant frequency.

±50% in 10% increments. The frequency of the reference model is calculated as

$$\omega_{nm} = \alpha\omega_{np} \qquad 0.5 \leq \alpha \leq 1.5 \qquad (12)$$

where α is a measure of the difference between the natural frequencies of the reference model and the actual system. In addition to the natural-frequency difference, the reference model has 10% damping ($\zeta_m = 0.1$), whereas the actual system has only 0.06% damping.

Experimental Setup

The experimental system is connected to an IBM AT computer with a digital signal processor (DSP) board (TMS320C30 System Board by Spectrum Signal Processing, Inc.) used to implement the control law. The structure is given an initial displacement (0.013 in.) and then released. Velocity and displacement sensors send information to the DSP board where the reference model and control gain equations are being integrated [see Eqs. (1–6)]. The system is allowed to vibrate freely for approximately 2 s (which we will call the settling period), which allows unmodeled high-frequency transients caused by the inductance in the actuator to decay (see Fig. 3). It was observed that the maximum force was a function of the settling period, so each test was run at a settling period causing the largest maximum force. After this initial settling period, the instantaneous velocity and displacement of the mass are used as initial conditions for the reference model, and the controller is started. Control commands are calculated and sent to the actuators, which apply the required forces to the structure, causing it to behave like the reference model. The sampling rate for the controller was 500 Hz.

Results

Figure 4 shows velocity responses of the actual system and the reference model for three values of the reference model frequency (controller was turned on at $t = 0$). As expected, MRAC does an excellent job at forcing the actual structure to follow the reference model. However, Table 1 shows that increasing the difference between the reference model and the actual system increases both the maximum force ($U_{p,\max}$) and the control effort CE. Defining the magnification factors as $U_{p,\max}/(U_{p,\max})_{\alpha=1}$ and $\mathrm{CE}/(\mathrm{CE})_{\alpha=1}$, Fig. 5 shows the magnification factors of these two quantities as a function of the difference between the reference model and the structure. Experimentally, Fig. 5a shows that for $\alpha = 0.5$, $U_{p,\max}$ is increased by a factor of 4.1, whereas a 50% error on the high side, ($\alpha = 1.5$) causes $U_{p,\max}$ to increase by a factor of 6. The analytical magnification factors are similar. Figure 5b shows a similar trend for the total control effort. Experimentally, Fig. 5b shows at $\alpha = 0.5$ the control effort is increased by a factor of 8.1, whereas analytical results show a factor of 9.1 increase. These large magnification factors show that the control effort is sensitive to differences between the plant and the reference model. Similar analytical results were obtained for a more complex structure in Refs. 11 and 12.

Table 1 Comparison of experimental and analytical maximum force and total control effort

	Maximum force, lb		Control effort, lb-s$^{1/2}$	
Alpha	Experiment	Theory	Experiment	Theory
0.5	0.127	0.168	0.0616	0.0854
0.6	0.102	0.131	0.0399	0.0550
0.7	0.086	0.096	0.0255	0.0346
0.8	0.050	0.038	0.0145	0.0134
0.9	0.034	0.026	0.0088	0.0099
1.0	0.031	0.028	0.0076	0.0089
1.1	0.031	0.037	0.0081	0.0106
1.2	0.041	0.060	0.0117	0.0177
1.3	0.070	0.089	0.0192	0.0262
1.4	0.135	0.122	0.0275	0.0353
1.5	0.186	0.162	0.0367	0.0449

The test results presented in Fig. 5a were obtained at a required damping ratio of 10%. It was also of interest to see what effect increasing or decreasing the damping in the reference model would have on the control costs. Experimental results for the effect of increasing or decreasing reference model damping on maximum force when using MRAC are shown in Fig. 6; analytical results showed similar trends. From this figure it can be seen that, with no frequency difference between the plant and the reference model ($\alpha = 1$), requiring more damping in the reference model has the expected effect of increasing the maximum force and control effort. However, when there are substantial differences in frequency between the reference model and the plant ($\alpha = 0.5$ and $\alpha = 1.5$), increased damping has the opposite effect. For example, when $\alpha = 1.5$, the maximum control force required to achieve 2.5% damping is 1.5 times larger than required to achieve 20% damping. The increase in control effort is even more dramatic, with the control effort required for 2.5% damping being 3.7 times larger than for 20% damping. Similar trends can be seen for $\alpha = 0.5$.

Although this result is somewhat counterintuitive, one possible explanation follows. For low required damping, the controller adds energy to force the frequency of the plant to match the frequency of the reference model and, at the same time, removes energy to provide the required damping. As required damping increases, the energy required to force the frequencies to match is reduced, whereas the energy that must be removed to damp the structure increases only slightly. The dependence on damping is a useful result in that, for a given design, if the objective was to reduce the control forces, one approach likely to be considered would be to reduce the damping requirements. However, from Fig. 6 it is seen that, when substantial frequency differences exist, this may have the opposite effect.

Optimizing the Weighting Matrices

As shown above, reasonable differences between the reference model and the actual plant can cause large increases in the magnitude of control effort and maximum force $U_{p,\max}$ required to force the plant to follow the reference model. It is desirable to minimize the effect of these differences by varying any available design parameters in the adaptive control law. In the following section it is shown that significant reductions in maximum force can be achieved by optimizing the T and T^* matrices. This is demonstrated analytically and experimentally for the suspended-mass system. However, improvements in maximum force are meaningful only if they do not degrade the performance of the MRAC in terms of following the reference model.

Measure of Fit for Suspended-Mass System

To maintain or improve plant-following performance (fit), it was necessary to quantify how well the plant follows the reference

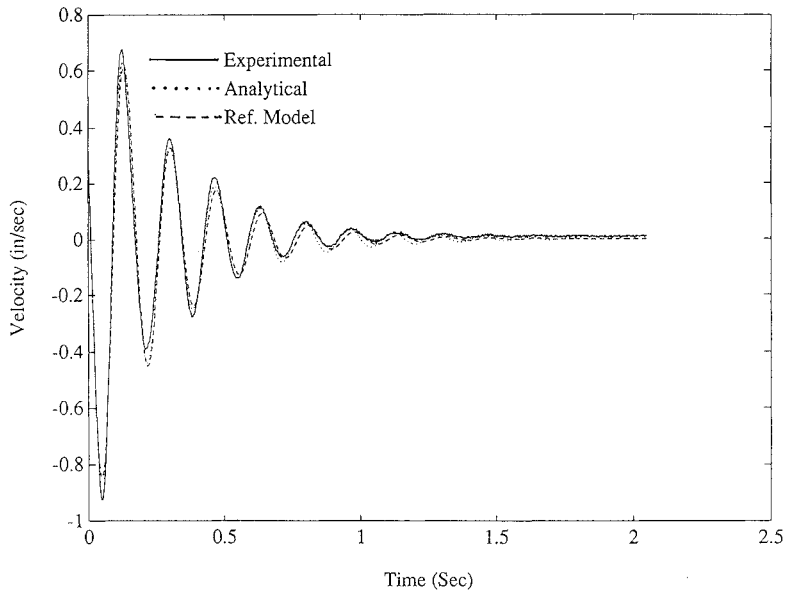

a)

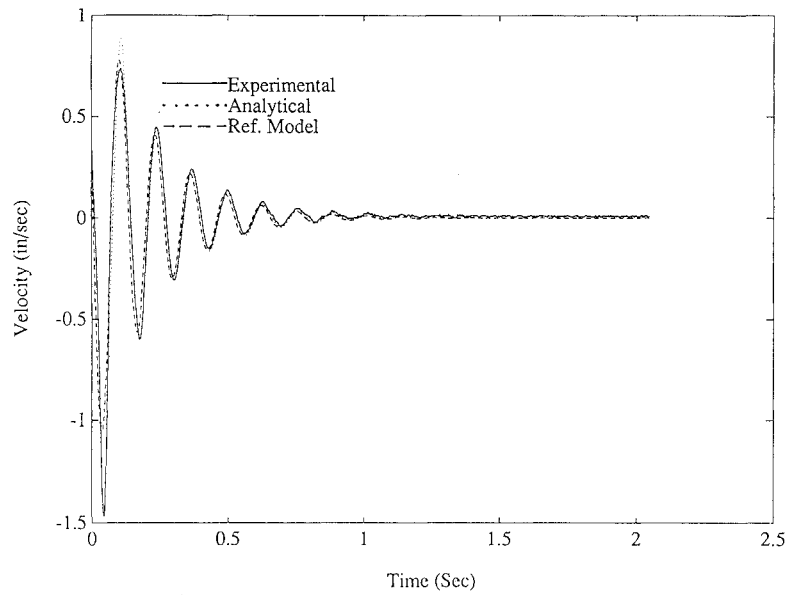

b)

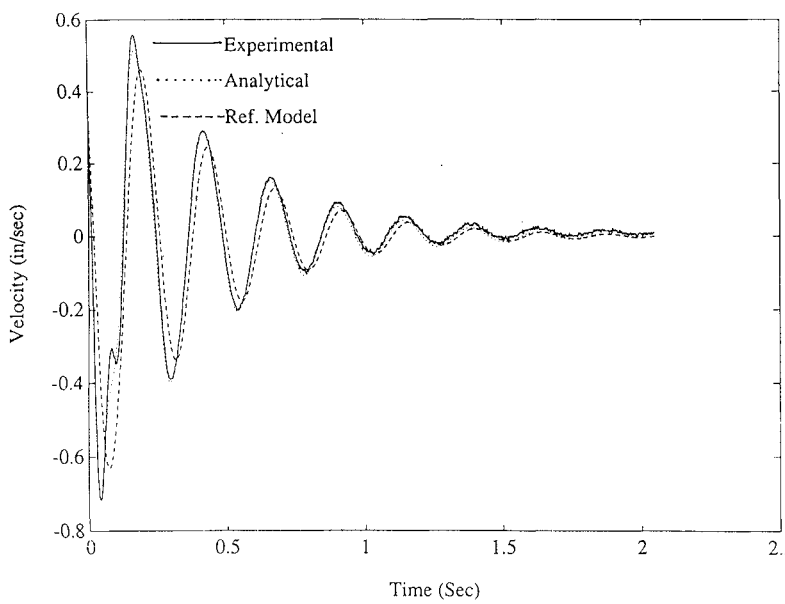

c)

Fig. 4 Comparison of experimental and analytical velocity response: a) $\omega_{nm} = 1.0\omega_{nm}$, b) $\omega_{nm} = 1.3\omega_{nm}$, and c) $\omega_{nm} = 0.7\omega_{nm}$.

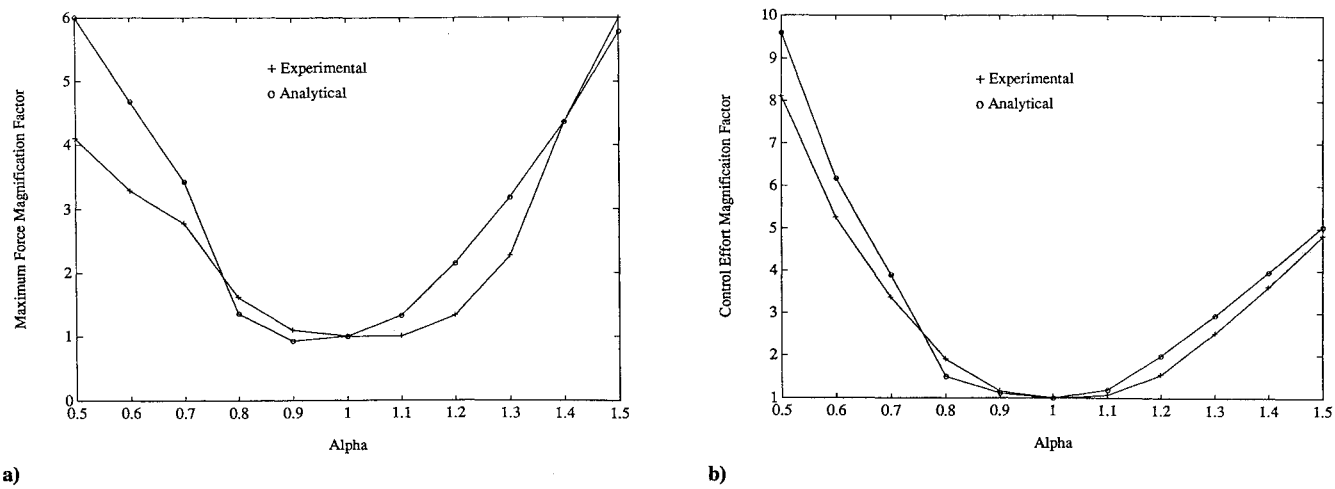

Fig. 5 Comparison of analytical and experimental factors: a) maximum force magnification and b) control effort magnification.

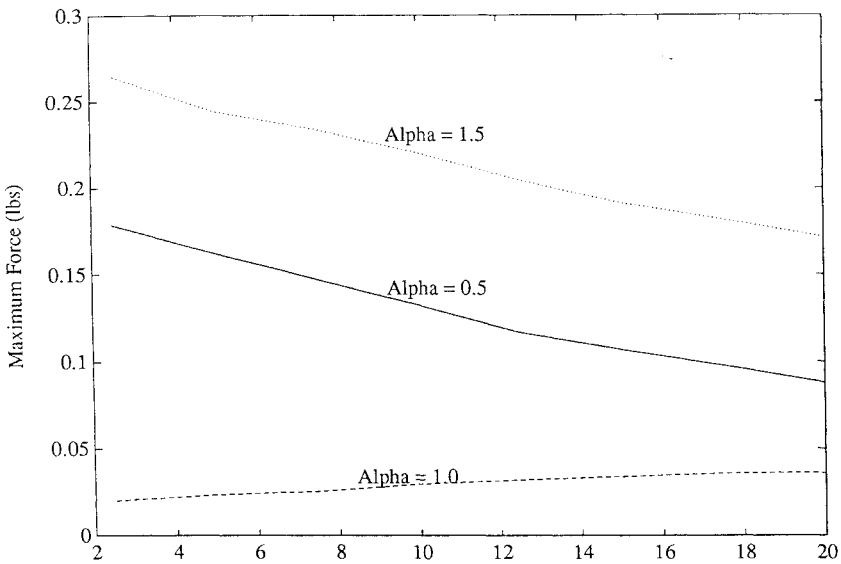

Fig. 6 Experimental effect of damping on maximum force for varying amounts of frequency difference.

model. In developing a fit parameter, two types of discrepancies between the plant and the model were considered. The first was the commonly used average amplitude difference, and the second was the less common phase difference between the two time traces. The advantage of shifting time traces can be understood by studying Fig. 4c. If only the vertical difference between the two damped sine waves is considered, two waves having the same magnitude, frequency, and damping ratios but a small phase difference would appear to have a poor fit when, in reality, the fit is quite good. Obviously, though, there should be some penalty associated with the need to apply the phase difference to achieve a good fit. Thus, the measure of fit was defined as

$$f = \min_{t_d} \left[\int_{t_0}^{t_f} |V_p(t) - V_m(t + t_d)| \, dt \right] + \eta |t_d| \qquad (13)$$

where t_d is the time shift that minimizes the integral of the difference between the plant velocity V_p and model reference velocity V_m, t_0 and t_f are the start and stop times of the controller, and η is a phase difference penalty factor chosen by the designer. For the suspended mass, t_d was found to occur between -0.06 to 0.06 s, and η was selected as 0.5 in./s.

Optimization Formulation

From Eqs. (4–6), it can be seen that the only parameters controlled by the designer are the T and T^* matrices. Furthermore, since the input to the reference model is zero, the fourth row and column of T and T^* have no effect on the controller. Therefore only nine matrix elements are specified by the designer. Using optimization for MRAC is limited because the error in any real application is unknown. In the present application, the optimizer uses $\alpha = 0.5, 1.5$ for limits on the modeling errors. These limits, reflecting 50% difference in frequency, are substantial, but they may not account for all modeling errors. Therefore, the designer should realize the optimal design may eventually predict unrealizable improvements. Even with the suspended-mass system (a very simple structure), this phenomenon is observed. The optimizer is given accurate values for the upper and lower bounds on the frequency, but other differences that occur because of the digital implementation are neglected. As will be seen, the experimental and analytical correlation remains good for the initial optimal design, but experimental and analytical correlation is lost as the optimal design evolves. We want to design the weighting matrices so the control effort is low over the range of possible frequency differences for the suspended-mass system. Based on Figs. 7a and 7b we assume the worst case will be either $\alpha = 0.5$ or $\alpha = 1.5$. The optimization problem is formulated as

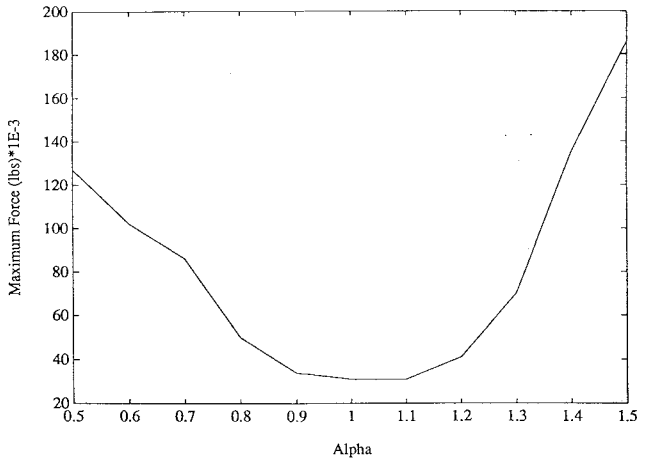

a)

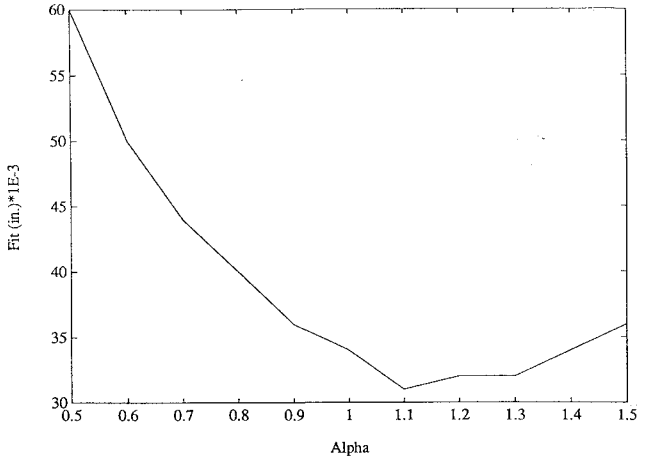

b)

Fig. 7 a) Experimental maximum force and b) experimental fit for different values of alpha; $T = 50[I]$, $T^* = [I]$.

follows: Find T, T^*, and $F_{\max}$ to minimize $F_{\max}$ such that

$$g_1(x) = f_{\max} - f(\alpha = 0.5) \geq 0 \tag{14}$$

$$g_2(x) = f_{\max} - f(\alpha = 1.5) \geq 0 \tag{15}$$

$$g_3(x) = F_{\max} - U_{p,\max}(\alpha = 0.5) \geq 0 \tag{16}$$

$$g_4(x) = F_{\max} - U_{p,\max}(\alpha = 1.5) \geq 0 \tag{17}$$

The worst fit allowable is $f_{\max}$ and was chosen to be 0.06 in. Here $F_{\max}$ is the larger of $U_{p,\max}(\alpha = 0.5)$ and $U_{p,\max}(\alpha = 1.5)$. Note that $F_{\max}$ is both a design variable and the objective function. This device is used because $F_{\max}$ takes on the largest of two values and therefore is not a smooth function; including $F_{\max}$ as a design variable avoids this problem. The optimization procedure (IMSL subroutine DNOONF, Ref. 13) uses a sequential quadratic programming algorithm and a finite difference gradient. After some experimentation with step sizes, derivatives of the objective function and constraints were calculated with a forward difference step size of 10^{-4}.

Optimization Results Using Only Diagonal Elements

As a start, we checked whether the design with scalar matrices $T = 50I$ and $T^* = I$, obtained by a rough experimental optimization for $\alpha = 1.0$, can be improved for the range $0.5 \leq \alpha \leq 1.5$. The matrices T and T^* were first defined as $T = \gamma_1 I$ and $T^* = \gamma_2 I$, with γ_1 and γ_2 as design variables. The initial values for the design variables were $\gamma_1 = 50.0$, and $\gamma_2 = 1.0$. Table 2, case 1, shows the optimal design $\gamma_1 = 14.24$ and $\gamma_2 = 1.143$ and compares analytical values with experimental results. The optimizer reduced the analytical $F_{\max}$ by 20%, while improving the fit slightly. Experimental results show a 24% decrease in $F_{\max}$ while preserving $f(\alpha = 0.5) = 0.06$ and losing only a small amount of fit at $\alpha = 1.5$, $f(\alpha = 1.5) = 0.044$.

Case 2 allowed T and T^* to be general diagonal matrices using the optimum of case 1 as the initial design. Table 2 shows that the optimizer changed the diagonal elements of T^*, but neither $F_{\max}$ nor f changed significantly. Experimental results showed the same lack of improvement.

Table 2 Initial and optimal designs for diagonal elements of T and T^* matrices

Possible design variables and performance measures	Case 1, scalar matrices		Case 2, diagonal matrices	
	Initial design	Optimal design	Initial design	Optimal design
γ_1	50.0[a]	14.24	1.0	1.0
γ_2	1.0[a]	1.143	1.0	1.0
$T(1, 1)$	1.0	1.0	14.244[a]	14.244
$T(2, 2)$	1.0	1.0	14.244[a]	14.244
$T(3, 3)$	1.0	1.0	14.244[a]	14.244
$T^*(1, 1)$	1.0	1.0	1.143[a]	0.996
$T^*(2, 2)$	1.0	1.0	1.143[a]	1.192
$T^*(3, 3)$	1.0	1.0	1.143[a]	1.144
$U_{p,\max}{}^{b}(\alpha = 0.5)$	0.129	0.100	0.100	0.100
$U_{p,\max}(\alpha = 0.5)$	0.161	0.126	0.126	0.126
$f^{b}(\alpha = 0.5)$	0.061	0.060	0.060	0.060
$f(\alpha = 0.5)$	0.064	0.060	0.060	0.060
$U_{p,\max}{}^{b}(\alpha = 1.5)$	0.185	0.140	0.140	0.140
$U_{p,\max}(\alpha = 1.5)$	0.151	0.128	0.128	0.128
$f^{b}(\alpha = 1.5)$	0.032	0.044	0.044	0.044
$f(\alpha = 1.5)$	0.028	0.027	0.027	0.027

[a]Variable used as design variable in optimization.
[b]Value obtained experimentally.

Table 3 Initial and optimal designs with off-diagonal elements of T and T^* matrices: case 3

Possible design variables	Initial design	Optimal design
γ_1	1.00	1.00
γ_2	1.00	1.00
$T(1, 1)$	14.244[a]	22.727
$T(1, 2)$	0	0
$T(1, 3)$	0	0
$T(2, 1)$	0	0
$T(2, 2)$	14.244[a]	8.710
$T(2, 3)$	0	0
$T(3, 1)$	0	0
$T(3, 2)$	0	0
$T(3, 3)$	14.244[a]	14.284
$T^*(1, 1)$	0.996[a]	1.767
$T^*(1, 2)$	0[a]	−1.408
$T^*(1, 3)$	0	0
$T^*(2, 1)$	0[a]	−1.408
$T^*(2, 2)$	1.192[a]	1.725
$T^*(2, 3)$	0	0
$T^*(3, 1)$	0	0
$T^*(3, 2)$	0	0
$T^*(3, 3)$	1.144[a]	1.265

[a]Variable used as design variable in optimization.

Optimization Results Using Off-Diagonal Elements

Next we evaluated the derivatives of the objective function with respect to each off-diagonal element in the T and T^* matrices for the optimum design of case 1. The parameters $T^*(1, 2)$ and $T^*(2, 1)$ have the largest derivatives and thus were selected for inclusion in the design variables list. Case 3 (Table 3) includes all diagonal elements of T and T^*, and off-diagonal elements $T^*(1, 2)$ and $T^*(2, 1)$ as design variables. Table 4 shows that by adding these two off-diagonal

Table 4 Experimental and analytical comparison of the maximum force and fitness ($\alpha = 0.5$)

	Experimental				Analytical			
	F_{max}, $\times 10^{-3}$ lb		Fit, $\times 10^{-3}$ in.		F_{max}, $\times 10^{-3}$ lb		Fit, $\times 10^{-3}$ in.	
Case	$\alpha = 0.5$	$\alpha = 1.5$	$\alpha = 0.5$	$\alpha = 1.5$	$\alpha = 0.5$	$\alpha = 1.5$	$\alpha = 0.5$	$\alpha = 1.5$
Initial design	129	185	61	32	161	151	64	28
1	100	140	60	44	126	128	60	27
2	100	140	60	44	126	128	60	27
3	92	191	60	39	104	105	60	18

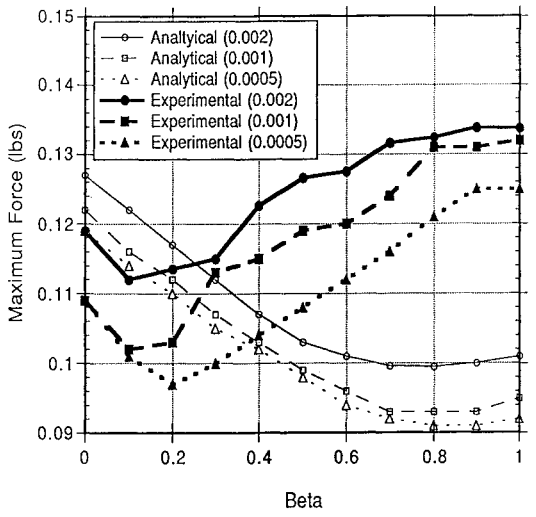

Fig. 8 Experimental and analytical maximum force for varying sizes of off-diagonal elements $T^*(1, 2)$ and $T^*(2, 1)$ and sampling rates ($\alpha = 1.5$).

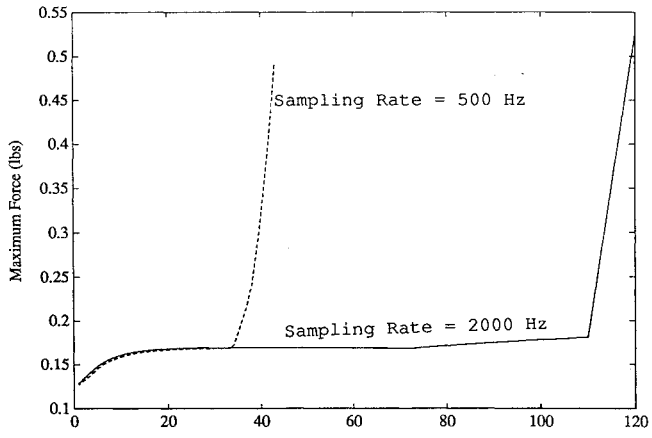

Fig. 9 Analytical maximum force for different diagonal $T = 18[I]$, $T^* = \lambda[I](\alpha = 1)$.

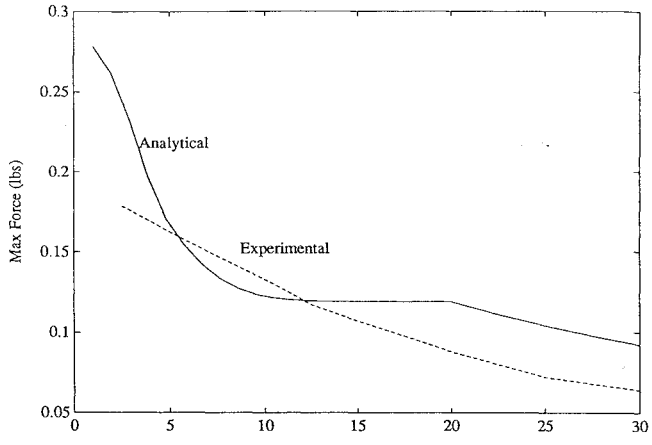

Fig. 10 Experimental and analytical effects of damping on the maximum force ($\alpha = 0.5$, T and T^* from optimal design case 2).

elements the optimization can reduce F_{max} by an additional 18% without increasing the fit parameters. However, experimentally this same design increases $F_{max}(\alpha = 1.5)$ by 36% from 0.14 to 0.191 lb. After some searching for the cause of the discrepancy we identified the sampling rate as a major contributor. We increased the sampling rate of the DSP board from 500 Hz (0.002 s/cycle) to 1000 Hz (0.001 s/cycle) and finally to 2000 Hz (0.0005-s/cycle). Figure 8 shows maximum force results, at the three sampling rates, for several designs with increasing off-diagonal elements. For $\beta = 0$, the T and T^* matrices are the optimal design of case 2. As β increases from 0 to 1, the $T^*(1, 2)$ and $T^*(2, 1)$ elements are increased linearly until, at $\beta = 1$, $T^*(1, 2) = T^*(2, 1) = -1.408$.

Figure 8 shows that, for $\alpha = 1.5$, the value of β where the analytical and experimental $U_{p,max}$ begin to diverge increases as the sampling rate gets higher. For a rate of 500 Hz (0.002 s/cycle) the experimental trends follow the analytical trends only for $\beta \leq 0.1$, and the maximum force is smaller than the $\beta = 0$ case only for $\beta \leq 0.35$. For the 2000-Hz (0.0005-s/cycle) case experimental trends follow analytical trends for $\beta \leq 0.2$, and the maximum force is less than the $\beta = 0$ case for $\beta \leq 0.5$. The $\alpha = 0.5$ case shows similar trends for $U_{p,max}$.

In Fig. 8, it is observed that almost all the improvement between experimental and analytical correlation came as a result of improvement in the experimental results. This suggests that the off-diagonal elements introduce some type of high-frequency motion or control transients into the system that the analysis does not model. However, from Fig. 8 it can also be seen that for $\beta = 0$ (zero on the off-diagonal elements) changing the sampling rate from 500 to 1000 Hz reduced F_{max} by 8.4%. This is a significant reduction since 500 Hz was already 41 times the Nyquist frequency. The importance of the sampling rate can also be seen from Fig. 9, where the maximum force as a function of T^* is plotted for sampling rates of 500 and 2000 Hz. It is seen that the point at which F_{max} diverges can be postponed from $T^* = 35I$ to $T^* = 110I$ by increasing the sampling rate.

Effects of Required Damping on Optimal Diagonal Design

Because of the previously observed effects that increased damping had on maximum force as frequency difference between the reference model and plant increased, it was desirable to check the optimum design. Optimal values from case 2 were selected for T and T^*, and reference model damping was increased. Figure 10 shows both analytically and experimentally that the trend to decrease maximum force as damping is increased was also seen for the optimal values of T and T^*.

Concluding Remarks

The performance of MRAC was studied in numerical simulations and verified experimentally on a single-degree-of-freedom system to understand how differences between the plant and the reference model affect the control effort. Good experimental and analytical agreement was demonstrated in control experiments, and it was

found that MRAC does an excellent job of controlling the structure and achieving the desired performance even when large differences between the plant and reference model exist. However, for the single-degree-of-freedom system used in this work reasonable differences between the reference model and the plant significantly increased both the required control effort and the maximum required force. Although the increase in control effort and maximum control force is not surprising, the size of the increase is.

It was shown that requiring the controller to provide more damping can actually decrease the required maximum force when differences between the plant and reference model exist. This result is very useful because one of the first attempts to counteract the increased maximum force due to differences between the plant and reference model might be to require less damping, which may actually increase the maximum control force.

Finally, optimization of weighting matrices was found to help reduce the increase of required control effort. However, eventually the optimization resulted in a design that required a sampling rate 40–80 times the Nyquist frequency for successful realization.

Acknowledgment

This work was supported in part by NASA Grant NAG1-224, Howard Adelman, Technical Monitor.

References

[1]Sobel, K., Kaufman, H., and Mabius, L. "Implicit Adaptive Control Systems for a Class of Multi-Input Multi-Output Systems," *IEEE Transactions on Aerospace and Electronics Systems*, Vol. AES-18, No. 5, 1982, pp. 576–590.

[2]Bar-Kana, Kaufman, H., and Balas, M., "Model Reference Adaptive Control of Large Structural Systems," *Journal of Guidance, Control, and Dynamics*, Vol. 6, No. 2, 1983, pp. 112–118.

[3]Mufti, H., "Model Reference Adaptive Control for Large Structural Systems," *Journal of Guidance and Control*, Vol. 10, No. 5, 1987, pp. 507–509.

[4]Ih, C.-H. C., Bayard, D. S., and Wang, S. J., "Space Station Adaptive Payload Articulation Control," *Proceedings of the Fourth IFAC Symposium on Control of Distributed Parameter Systems*, Los Angeles, CA, July 1986, pp. 253–261.

[5]Bayard, D. S., Ih, C.-H. C., and Wang, S. J., "Adaptive Control for Flexible Structures with Measurement Noise," *Proceedings of the American Control Conference* (Minneapolis, MN), June 10–12, 1987, pp. 368–379.

[6]Sundararajan, N., Williams, J. P., and Montgomery, R. C., "Adaptive Modal Control of Structural Dynamic Systems Using Recursive Lattice Filters," *Journal of Guidance and Control*, Vol. 8, No. 2, 1985, pp. 223–229.

[7]Ih, C.-H. C., Bayard, D. S., Wang, S. J., and Elder, D. B., "Adaptive Control Experiment with a Large Flexible Structure," *Proceedings of the AIAA Guidance, Navigation, and Control Conference* (Minneapolis, MN), AIAA, Washington, DC, 1988, pp. 832–851; also AIAA Paper-88-4153.

[8]Ih, C.-H. C., Bayard, D. S., Ahmed, A., and Wang, S. J., "Experiments in Multivariable Adaptive Control of a Large Flexible Structure," *Proceedings AIAA Guidance, Navigation and Control Conference* (Boston, MA), AIAA, Washington, DC, 1989, pp. 1207–1217.

[9]Chiang, W.-W., and Cannon, R. H., Jr., "The Experimental Results of a Self-Tuning Adaptive Controller Using Online Frequency Identification," *Journal of the Astronautical Sciences*, Vol. 33, No. 1, 1985, pp. 71–83.

[10]Boussalis, D., Bayard, D. S., Ih, C.-H. C., Wang, S. J., and Ahmed, A., "Experimental Study of Adaptive Pointing and Tracking for Large Flexible Space Structures," *Proceedings of the Guidance, Navigation and Control Conference* (New Orleans, LA), AIAA, Washington, DC, 1991, pp. 769–778; also AIAA Paper 91-2691.

[11]Messer, R. S., Haftka, R. T., and Cudney, H. H., "Analytical and Experimental Study of Control Effort Associated with Model Reference Adaptive Control," *Proceedings of the 33rd Structures, Structural Dynamics, and Materials Conference* (Dallas, TX), AIAA, Washington, DC, 1992, pp. 1568–1579; also AIAA Paper 92-2320.

[12]Messer, R. S., Haftka, R. T., and Cudney, H. H., "The Cost of Model Reference Adaptive Control: Analysis, Experiments, and Optimization," *Proceedings of the 34th Structures, Structural Dynamics and Materials Conference* (La Jolla, CA), AIAA, Washington, DC, 1993, pp. 3115–3125; also AIAA Paper 93-1658.

[13]IMSL Math/Library, *Fortran Subroutines for Mathematical Applications Version 1.1*, Dec. 1989, pp. 895–901.